CrossMark
click for updates

Synthesis of 2-styrylchromones: *In vitro* and *in silico* anticancer activity evaluation

Brilliana Via Safitri, Alfinda Novi Kristanti[*], Hery Suwito, Kautsar Ul Haq, Dicky Hendriyanto
Department of Chemistry, Faculty of Science and Technology, Universitas Airlangga, Surabaya, Indonesia.

ARTICLE INFO	**ABSTRACT**
	The efforts to obtain cancer drugs are still a topic of many research studies considering that cancer is one of the main causes of human death. 2-Styrylchromones are a group of compounds with potential anticancer activity. This research was conducted to synthesize some 2-styrylchromones which involved the formation of 2-methylchromone, followed by aldol condensation with various benzaldehydes. The compound structures were determined using spectroscopic methods, which included ultra violet-visible, Fourier-transform infrared, proton nuclear magnetic resonance, carbon nuclear magnetic resonance- attached proton test APT, and high-resolution mass spectrometry. The toxicity test of the synthesized compounds was carried out *in vitro* against Henrietta Lacks cancer cells and *in silico* by molecular docking of the human kinesin Eg5 receptor. The results showed that the synthesized compound substituted with three methoxy groups presented the best anticancer activity, both *in vitro* (inhibition 100%) and *in silico* tests (grid score −41,029 kcal/mol).

INTRODUCTION

Cancer is one of the leading causes of death worldwide. Therefore, research to find new compounds, both natural and synthetic, which can be used in cancer treatment, continues. From nature, we know vinblastine and vincristine have been used as anticancer drugs. Several synthesized compounds, from various groups of compounds, were also developed to provide potential and promising anticancer agents, including metal complexes (Ali *et al.*, 2013), some compounds with heterocyclic nuclei (Ali *et al.*, 2015), several classes of imidazoles (Ali *et al.*, 2017), styrylcromones (Momoi *et al.*, 2005) and so forth.

Styrylchromone, a compound with a C6-C5-C6 building block, is known to have various biological activities, such as antioxidant, anti-inflammatory, antimicrobial, antitumor, and neuroprotective activities. 2-Styrylchromones have a styryl group at position 2 in the chromone ring. Up until 2016, only nine derivatives had been isolated from some natural sources, such as

cryptophycean alga, *Chrysophaeum taylori*, *Imperata cylindrica*, Chinese eaglewood, *Platanus x acerifolia*, *Juniperus chinensis*, and *Dioscorea bulbifera* (Santos and Silva, 2017).

Therefore, 2-styrylchromone is rarely found in nature, and the provision of this compound must be carried out through the synthesis of organic compounds. One of the oldest approaches to the synthesis of 2-styrylchromones consists of base-promoted condensation between 2-methylchromones and benzaldehydes (Santos and Silva, 2017). Meanwhile, according to Bondge, chromones have been prepared from *o*-hydroxyacetophenones in three or more steps via either Allan Robinson's method or modified Kostanecki Robinson's procedure (Bondge *et al.*, 2009).

In our study, we synthesized some 2-strylchromones, the structure of which is presented in Table 1. The synthesis occurred in two steps: first, the formation of 2-methylchromone (3) from 2-hydroxyacetophenone (1) through the formation of 2-hydroxy-2-methylchromanone (2), followed by aldol condensation with various benzaldehydes. The reaction is shown in Figure 1.

The toxicity test of the synthesized compound was carried out by MTT method against Henrietta Lacks (HeLa) cancer cells and the *in silico* test was carried out using the human kinesin Eg5 receptor, a potential drug target for the development of

*Corresponding Author
Alfinda Novi Kristanti, Department of Chemistry, Faculty of Science and
Technology Universitas Airlangga, Surabaya, Indonesia.
E-mail: alfinda-n-k @ fst.unair.ac.id

Table 1. 2-Styrylchromones synthesized.

Code	R	Structure	Name of compound (International Union of Pure and Applied Chemistry)
4a	H		(*E*)-2-styryl-4H-chromen-4-one
4b	4-Cl		(*E*)-2-(4-chlorostyryl)-4H-chromen-4-one
4c	4-Br		(*E*)-2-(4-bromostyryl)-4H-chromen-4-one
4d	2,5-diCl		(*E*)-2-(2,5-dichlorostyryl)-4H-chromen-4-one
4e	2,3-diOCH₃		(*E*)-2-(2,3-dimethoxystyryl)-4H-chromen-4-one
4f	2,5-diOCH₃		(*E*)-2-(2,5-dimethoxystyryl)-4H-chromen-4-one
4g	3,4,5-triOMe		(*E*)-2-(3,4,5-trimethoxystyryl)-4H-chromen-4-one
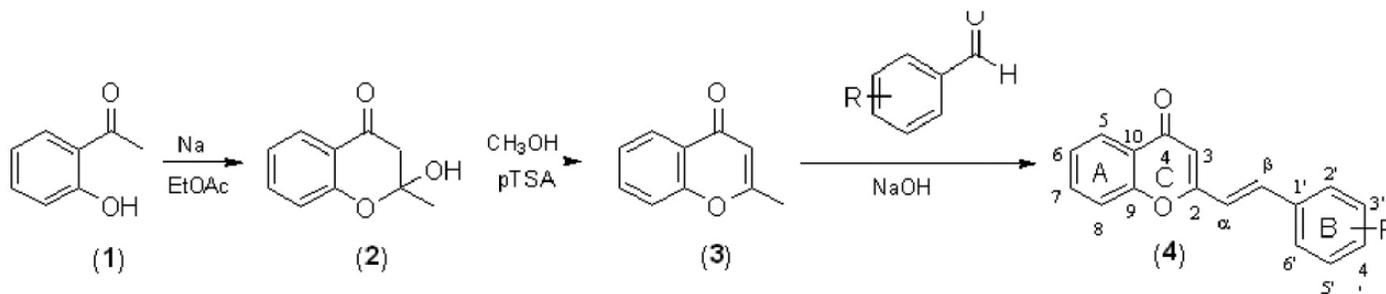
Figure 1. Reaction of 2-styrylchromones synthesis.

cancer chemotherapy. The most sophisticated Eg5 targeting agent is ispinesib, which exhibits strong anticancer activity (Talapatra *et al.*, 2012).

MATERIALS AND METHODS

Materials

Ethyl acetate, sodium, 2′-hydroxyacetophenone, HCl 0.5 N, methanol, *p*-toluene sulfonic acid (*p*TSA), benzaldehyde, 4-chlorobenzaldehyde, 4-bromobenzaldehyde, 2,5-dichlorobenzaldehyde, 2,3-dimethoxybenzaldehyde, 2,5-dimethoxybenzaldehyde, 3,4,5-trimethoxybenzaldehyde, distilled water, ethanol, and NaOH 40% were used. For 3-(4,5-dimethylthiazol-2-yl)-2,5-diphenyltetrazolium bromide (MTT) assay, MTT reagent, media culture, HeLa cell lines, trypan blue, and ethanol 70% were needed.

Apparatus

Three-neck round bottom flasks, reflux, thermometer, a set of thin layer chromatography tools, hot plates, stands, clamps, micropipettes, Buchner funnels, and Fisher–Johns melting point apparatus were used. The instruments used for structural elucidation of compounds were ultra violet-visible (UV-Vis) spectrophotometers (Shimadzu UV-1800), Fourier Transform Infrared (FTIR) spectrophotometer (Shimadzu IR Tracer-100), NMR spectrometer (JEOL JNM-ECS 400), and mass spectrometer (JEOL 600H-1).

Synthesis

Synthesis of 2-methylchromone (3)

A solution of 2′-hydroxyacetophenone (**1**) (3 mmol), 10 ml of ethyl acetate, and 0.33 g of sodium was put into a three-neck round bottom flask and stirred with a magnetic stirrer for 23 hours at a temperature of 28°C–30°C. HCl 0.5 N was added dropwise for 4.2 ml until a yellow precipitate was formed. This reaction yielded two compounds: 4-methylcoumarine (**5**) and 2-hydroxy-2-methylchromanone (**2**). After these two compounds were formed, the next step (synthesis of 2-methylchromone) was carried out to use the two mixture compounds as reactants. Thus, 356 mg of the mixture was reacted with 0.25 mmol of *p*TSA in 14 ml of methanol under stirring and heating at 100°C for 2 hours. The product obtained was purified by silica gel column chromatography using chloroform-n-hexane mixture as eluent. The product desired was eluted by chloroform : n-hexane in a ratio of 3:1.

Synthesis of 2-styrylchromones (4a–4g)

2-Methylchromone (**3**) (0.5 mmol) obtained from the previous step and various benzaldehydes (0.55 mmol) were dissolved in 8 ml ethanol. Then, 0.5 ml of 40% NaOH was added drop by drop into the mixture and then stirred with a magnetic stirrer for 1 hour below 5°C. After 1 hour, the mixture was stirred at room temperature for 3 hours and cold distilled water was then added to form a precipitate. The mixture was filtered using a Buchner funnel to give a yellow solid.

Cytotoxicity screening on HeLa cells

The synthesized compounds were tested for their cytotoxicity against HeLa cancer cells using the MTT method. This test was carried out by planting cancer cell cultures incubated 24 hours into a 96-well plate with a HeLa cell concentration of 6×10^4 cells/100 µl. The media in the well were removed for further addition of 200 µl synthesized compound with a concentration of 30 µM and incubated for 48 hours at 37°C. In addition to the synthesized compound as a test compound, there is also doxorubicin as a positive control, a cell control solution consisting of culture media and cells as a negative control, and a media control solution consisting of culture media as a blank. After incubating for 48 hours, the media were removed for further administration of MTT reagents (0.5 mg/ml) of 200 µl into each well. Subsequently, incubated again for 3–4 hours, formazan crystals were formed. After the formazan crystals from the MTT reduction were formed, the media were removed from the plate and dissolved in 100 µl DMSO on each plate to read the absorbance value with an ELISA reader at a wavelength of 570 nm. After absorbance the data were obtained, then the percentage of inhibited cells was determined (Essien *et al.*, 2016):

$$\% \text{ Inhibition} = 100 - \frac{\text{OTC} - \text{ONC}}{\text{OPC} - \text{ONC}} \times 100$$

OTC is OD of test compound, ONC is OD of negative control, and OPC is OD of positive control.

Docking studies on Eg5 human kinesin protein

The program used in this experiment for docking was Dock6. Eg5 protein complex with ispinesib ligand was downloaded from the Protein Data Bank (PDB) with 4AP0 access code and the A chain was separated using USCF Chimera 1.11.2. RMSD obtained in this study was 0.34 Å. The ligand used for docking was synthesized compounds (**4a–4g**). The ligand structure was obtained by drawing on the ChemDraw Ultra 12.0 program and then stored in *.mol format and opened with Gaussian 09W for geometry optimization with the DFT basis set B3LYP/6-31G** method (Yadava *et al.*, 2011). After geometry optimization, the file was opened in the USCF Chimera 1.11.2 program to add hydrogen (add hydrogen) and charge (add charge) and then saved in *.mol format.

RESULTS AND DISCUSSION

Synthesis of 2-styrylchromones

In organic chemistry, Allan Robinson's reaction is the chemical reaction of *o*-hydroxyaryl ketones with an anhydride. During the reaction mechanism, a diketone was formed as an intermediate. In 2013, Zheng *et al.* (2013) succeeded in synthesizing a compound near-infrared fluorescent probe for H$_2$S. In the six steps of that synthesis reaction, there was the formation of 2-methylchromone from 2-hydroxyacetophenone. This reaction needed dry ethyl acetate, sodium, and diluted HCl. The intermediate compound formed in the reaction was a diketone 1-(2-hydroxyphenyl)butane-1,3-dione. Another probe was synthesized by Lu *et al.* (2016), which wrote the same mechanism for the formation of 2-methylchromone.

The other chromones' synthesis reaction is Kostanecki's acylation. The Kostanecki acylation is an acylation reaction of *o*-hydroxyaryl ketones with anhydrides, followed by cyclization. This reaction's mechanism consists of three well-differentiated reactions: phenol O-acylation with the formation of a tetrahedral intermediate, intramolecular aldol condensation to cyclize, and

formation of a hydroxydihydrochromone and elimination of the hydroxyl group to form the chromone (or coumarin).

    In our study, when 2′-hydroxyacetophenone was reacted with ethyl acetate and sodium, two compounds were formed. After elucidating the structures, there were 4-methylcoumarine **(5)** and 2-hydroxy-2-methylchromanone **(2)**, the structure of which was shown in Figure 2. So, in our study, the reaction mechanism did not correspond to what was reported by previous researchers (Lu *et al.*, 2016; Zheng *et al.*, 2013). A diketone was not formed, if not compound **(2)** was a major product.

    The existence of 4-methylcoumarine was assigned by the following signals in the proton nuclear magnetic resonance (1H-NMR) spectrum: proton signal of methyl group at δ_H 2.33 ppm (s, 3H), vinylic proton signal at δ_H 6.18 ppm (s, 1H), and four aromatic proton signals at 7.40 ppm (ddd, 8.0, 7.1, 1.1 Hz, 1H); 7.54 ppm (dd, 8.6, 1.1 Hz, 1H); 7.71 ppm (ddd, 8.6, 7.1, 1.7 Hz, 1H); and 7.94 ppm (dd, 8.0, 1.7 Hz, 1H). Meanwhile, the existence of 2-hydroxy-2-methylchromanone was assigned by the following signals: proton signal of methyl group at 1.97 ppm (s, 3H), proton signal of methylene group at 3.35 ppm (s, 2H), proton signal of hydroxyl group at 5.55 ppm, and four aromatic proton signals.

    After these two compounds were formed, the synthesis was continued to the next step using the mixture. This can be applied because the dehydration reaction occurred only on compounds **(2)**, which can be dehydrated under acidic and high temperature conditions. Meanwhile, compound **(5)** did not react. Besides, separating the two using chromatography seems difficult because they both have almost the same polarity. This dehydration reaction used *p*TSA as a catalyst, which resulted in a faster reaction time of 2 hours than hydrochloric acid, which took 30 hours. It is because *p*TSA is a strong organic acid that can dissolve and mix perfectly in this reaction condition. The TLC analysis of the reaction product showed two spots separated by silica gel column chromatography using chloroform-n-hexane mixture as the eluent.

    Then, 2-styrylchromones **(4a–4g)** were synthesized using aldol condensation between 2-methylchromone **(3)** and benzaldehyde appropriate. All synthesized compounds have two peaks in UV-Vis spectrum, where peak I appeared at a wavelength of 220–270 nm, which belonged to the benzoyl group, and peak II appeared in 300–390 nm which belonged to the extended cinnamoyl peak. On FTIR spectra, the absorption band appeared at the wavenumber (*v*) 1,610–1,630 cm^{-1} for the C=C conjugated alkene, 1,380–1,390 cm^{-1} for C_{aryl}–O–C_{vinyl} in the chromone ring, and 1,460–1,560 cm^{-1} for C=C of benzene. The ^{1}H NMR spectra provide information about signals that indicated the formation of
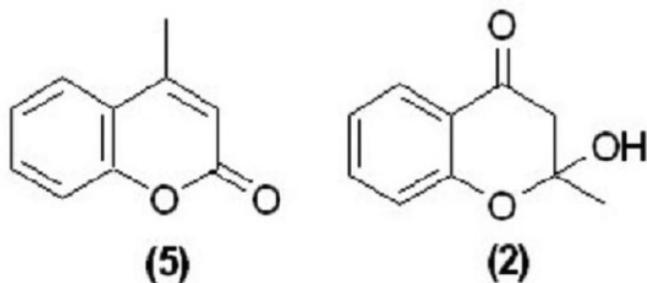
Figure 2. Structure of 4-methylcoumarine and 2-hydroxy-2-methylchromanone.

2-stirylchromone skeleton. Two doublet signals with a coupling constant of 16 Hz are the proton *trans*-ethylenic signals of H_α and H_β, which appeared at 6.75–6.84 ppm and 7.54–7.93 ppm, respectively. In ring A, the substituents are in the *ortho* position so that all the synthesized compounds showed the presence of four proton signals coupled to each other, producing dd and ddd multiplicity. The singlet signal, which was H_3 signals on the C ring, appeared at δ_H 6.32–6.55 ppm. At ^{13}C APT spectra, the most deshielding signal appeared at δ_C 170–200 ppm, which belonged to the carbonyl group. Analysis with high-resolution mass spectrometry (HRMS) provided information on the molecular formula according to the structure of the synthesized compounds.

2-Methylchromone (3)

    Yellow needle crystals. FTIR (DFR, KBr) *v* cm^{-1}: 3,070 (CH sp^2); 2,914, 2,951 (CH sp^3); 1,647 (C=O); 1,618 (Cα=Cβ); 1,477, 1,463, 1,442 (C=C aromatic); 1,371 (C_{aryl}–O–C_{vinyl}). ^{1}**H NMR** (400 MHz, CDCl$_3$) δ 8.17 (dd, *J* = 8.1 Hz, 1.7 Hz, 1H); 7.63 (ddd, *J* = 8.5 Hz, 7.1 Hz, 1.7 Hz, 1H); 7.41 (dd, *J* = 8.5 Hz, 1.1 Hz, 1H); 7.37 (ddd, *J* = 8.1 Hz; 7.1 Hz, 1.1 Hz, 1H); 6.18 (q, *J* = 0.7 Hz, 1H); 2.38 (d, *J* = 0.7 Hz, 3H). ^{13}**C NMR** (101 MHz, CDCl$_3$) δ 20.7; 110.6; 117.1; 123.6; 125.0; 125.7; 129.1; 133.6; 166.4; 178.4.

(E)-2-styryl-4H-chromen-4-one (4a)

    Yellow solid; m.p. = 138,3–139,7°C. **UV-Vis** (EtOH) λ_{max} (nm), log ε: 254 (3.64); 330 (4.42). FTIR (DFR, KBr, *v*) cm^{-1}: 3,057, 3,016 (CH sp^2); 1,656 (C=O); 1,614 (Cα=Cβ); 1,465, 1,477, 1,560 (C=C aromatic); 1,386 (C_{aryl}–O–C_{vinyl}). ^{1}**H NMR** (400 MHz, CDCl$_3$) δ 8.20 (dd, *J* = 7.9 Hz, 1.5 Hz, 1H); 7.69 (ddd, *J* = 8.5 Hz, 7.4 Hz, 1.5 Hz, 1H); 7.62 (d, *J* = 16 Hz, 1H); 7.59 (dd, *J* = 8.1 Hz, 1.2 Hz, 2H); 7.54 (dd, *J* = 8.5 Hz, 1.2 Hz, 1H); 7.41 (m, 3H); 7.40 (ddd, *J* = 7.9 Hz, 7.4 Hz, 1.2 Hz, 1H); 6.80 (d, *J* = 16 Hz, 1H); 6.37 (s, 1H). carbon nuclear magnetic resonance- attached proton test (13C NMR APT) (101 MHz, CDCl$_3$) δ 178.6, 161.9, 156.1, 137.2, 135.0, 133.9, 130.0, 129.1, 127.8, 125.8, 125.1, 124.1, 120.3, 118.0, 110.7. **HRMS** (M$^{+•}$) 248.0817 ($C_{17}H_{12}O_2$).

(E)-2-(4-chlorostyryl)-4H-chromen-4-one (4b)

    Yellow solid; m.p. = 214°C–216°C. UV-Vis (EtOH) λ_{max} (nm), log ε: 257 (4.05); 331 (4.51). FTIR (DFR, KBr, *v*) cm^{-1}: 3,032, 3,064 (C-H sp^2); 1,651 (C=O); 1,624 (C=C); 1,465, 1,475, 1,560 (C=C aromatic); 1,390 (C_{aryl}–O–C_{vinyl}); 1,091 (C–Cl). ^{1}**H NMR** (400 MHz, CDCl$_3$) δ 8.19 (dd, *J* = 8.0 Hz, 1.7 Hz, 1H); 7.68 (ddd, *J* = 8.7 Hz, 7.2 Hz, 1.7 Hz, 1H); 7.55 (d, *J* = 16 Hz, 1H); 7.52 (m, 1H); 7.51 (d, *J* = 8.6 Hz, 2H); 7.40 (ddd, *J* = 8.7 Hz, 7.2 Hz, 1.0 Hz, 1H); 7.39 (d, *J* = 8.6 Hz, 2H); 6.75 (d, *J* = 16 Hz, 1H); 6.32 (s, 1H). ^{13}**C NMR APT** (101 MHz, CDCl$_3$) δ 178.5; 161.4; 156.1; 135.8; 135.5; 133.9; 133.6; 129.4; 128.9; 125.8; 125.2; 124.2; 120.9; 117.9; 111.0. **HRMS** (M$^{+•}$) 282.0456 ($C_{17}H_{11}Cl O_2$).

(E)-2-(4-bromostyryl)-4H-chromen-4-one (4c)

    Yellow solid; m.p. = 210°C–211°C. UV-Vis (EtOH) λ_{max} (nm), log ε: 253 (3.89); 334 (4.53). FTIR (DFR, KBr, *v*) cm^{-1}: 3,032, 3,062 (CH sp^2); 1,649 (C=O); 1,624 (C=C); 1,465, 1,473, 1,566 (C=C aromatic); 1,390 (C_{aryl}–O–C_{vinyl}); 1,070 (C–Br). ^{1}**H NMR** (400 MHz, CDCl$_3$) δ 8.19 (dd, *J* = 7.9 Hz, 1.7 Hz, 1H); 7.68 (ddd, *J* = 8.6 Hz, 7.0 Hz, 1.7 Hz, 1H); 7.54 (d, *J* = 8.5 Hz, 2H); 7.53 (d, *J* = 16 Hz, 1H); 7.52 (dd, *J* = 8.1 Hz, 2.8 Hz, 1H); 7.44 (d; *J* = 8.5 Hz; 2H); 7.40

(ddd; *J* = 8.1 Hz, 7.9 Hz, 1.2 Hz; 1H); 6.77 (d, *J* = 16 Hz, 1H); 6.33 (s, 1H). **¹³C NMR APT** (101 MHz, CDCl₃) δ 178.5; 161.3; 156.0; 135.6; 134.0; 133.9; 132.3; 129.1; 125.8; 125.2; 124.2; 124.1; 121.0; 117.9; 111.0. **HRMS** (M⁺·) 325.9936 (C₁₇H₁₁Br O₂).

(E)-2-(2,5-dichlorostyryl)-4H-chromen-4-one (4d)

Yellow solid; m.p. = 197°C–198°C. UV-Vis (EtOH) λ$_{max}$ (nm), log ε: 248 (4.12); 325 (4.44). FTIR (DFR, KBr, *v*) cm⁻¹: 3,066 (C-H sp²); 1,647 (C=O); 1,635 (C=C); 1,465, 1,469, 1,560 (C=C aromatic); 1,388 (C$_{aryl}$–O–C$_{vinyl}$); 1,095 (C–Cl). **¹H NMR** (400 MHz, CDCl₃) δ 8.19 (dd, *J* = 8.0 Hz, 1.7 Hz, 1H), 7.91 (d, *J* = 16 Hz, 1H), 7.70 (ddd, *J* = 8.5 Hz, 7.2 Hz, 1.7 Hz, 1H), 7.67 (d, *J* = 2.4 Hz, 1H), 7.56 (dd, *J* = 8.5 Hz, 1.0 Hz, 1H), 7.40 (ddd, *J* = 8.0 Hz, 7.2 Hz, 1.7 Hz, 1H), 7.37 (d, *J* = 8.6 Hz, 1H), 7.27 (dd, *J* = 8.6 Hz, 2.4 Hz, 1H), 6.77 (d, *J* = 16 Hz, 1H), 6.38 (s, 1H). **¹³C NMR APT** (101 MHz, CDCl₃) δ 178.5; 160.8; 156.0; 134.7; 134.1; 133.3; 132.8; 131.5; 131.4; 130.5; 127.0; 125.8; 125.3; 124.1; 124.0; 118.1; 111.9. **HRMS** (M⁺·) 316.0051 (C₁₇H₁₀Cl₂O₂).

(E)-2-(2,3-dimethoxystyryl)-4H-chromen-4-one (4e)

Yellow solid; m.p. = 162°C–163°C. UV-Vis (EtOH) λ$_{max}$ (nm), log ε: 243 (4.09); 335 (4.81). **FTIR** (DFR, KBr, *v*) cm⁻¹: 3,043, 3,066 (CH sp²); 2,831, 2,935, 2,991 (CH sp³), 1,653 (C=O); 1,631 (C=C); 1,465, 1,477, 1,579 (C=C aromatic); 1,392 (C$_{aryl}$–O–C$_{vinyl}$); 1,271 (C$_{aryl}$–O–C$_{alkyl}$). **¹H NMR** (400 MHz, CDCl₃) δ 8.19 (dd, *J* = 7.9 Hz, 1.5 Hz, 1H); 7.93 (d, *J* = 16 Hz, 1H); 7.68 (ddd, *J* = 8.5 Hz, 7.1 Hz, 1.5 Hz, 1H); 7.57 (dd, *J* = 8.5 Hz, 1.1 Hz, 1H); 7.39 (ddd, *J* = 8.5 Hz, 7.9 Hz, 1.1 Hz, 1H); 7.23 (dd, *J* = 8.0 Hz, 1.2 Hz, 1H); 7.10 (t, *J* = 8.0 Hz, 1H); 6.95 (dd, *J* = 8.0 Hz, 1.2 Hz, 1H); 6.84 (d, *J* = 16 Hz, 1H); 6.35 (s, 1H); 3.92 (s, 3H); 3.91 (s, 3H). **¹³C NMR APT** (101 MHz, CDCl₃) δ 178.6; 162.1; 156.1; 153.2; 148.2; 133.8; 131.7; 129.3; 125.7; 125.1; 124.4; 124.2; 121.7; 118.8; 118.1; 113.6; 110.7; 61.5; 56.0. **HRMS** (M⁺·) 308.1037 (C₁₉H₁₆O₄).

(E)-2-(2,5-dimethoxystyryl)-4H-chromen-4-one (4f)

Yellow solid; m.p. = 158°C–159°C. UV-Vis (EtOH) λ$_{max}$ (nm), log ε: 261 (3.98); 321, (4.26); 380 (4.14). FTIR (DFR, KBr, *v*) cm⁻¹: 3,003 (CH sp²); 2,831, 2,904, 2,937 (CH sp³); 1,641 (C=O); 1,631 (C=C); 1,465, 1,492, 1,560 (C=C aromatic); 1,390 (C$_{aryl}$–O–C$_{vinyl}$); 1,222 (C$_{aryl}$–O–C$_{alkyl}$). **¹H NMR** (400 MHz, CDCl₃) δ 8.19 (dd, *J* = 8.0 Hz, 1.8 Hz, 1H), 7.89 (d, *J* = 16 Hz, 1H), 7.67 (ddd, *J* = 8.5 Hz, 7.2 Hz, 1.8 Hz, 1H), 7.55 (dd, *J* = 8.5 Hz, 1.2 Hz, 1H), 7.38 (ddd, *J* = 8.0 Hz, 7.2 Hz, 1.2 Hz, 1H), 7.11 (d, *J* = 2.7 Hz, 1H), 6.91 (dd, *J* = 8.7 Hz, 2.7 Hz, 1H), 6.87 (d, *J* = 8.7 Hz, 1H), 6.84 (d, *J* = 16 Hz, 1H), 6.33 (s, 1H), 3.90 (s, 3H), 3.83 (s, 3H). **¹³C NMR APT** (101 MHz, CDCl₃) δ 178.6; 162.4; 156.1; 153.7; 152.6; 133.7; 132.2; 125.7; 125.0; 124.6; 124.2; 121.0; 118.1; 116.6; 112.8; 112.5; 110.5; 56.2; 55.9. **HRMS** (M⁺·) 308.1050 (C₁₉H₁₆O₄).

(E)-2-(3,4,5-trimethoxystyryl)-4H-chromen-4-one (4g)

Yellow solid; m.p. = 201°C–202°C. UV-Vis (EtOH) λ$_{max}$ (nm), log ε: 251 (4.33); 357 (4.61). FTIR (DFR, KBr, *v*) cm⁻¹: 3,005 (CH sp²); 2,827, 2,845, 2,941, 2,974 (CH sp³), 1,631 (C=O); 1,614 (Cα=Cβ); 1,462, 1,504, 1,579 (C=C aromatic); 1,382 (C$_{aryl}$–O–C$_{vinyl}$); 1,128 (C$_{aryl}$–O–C$_{alkyl}$). **¹H NMR** (400 MHz, CDCl₃) δ 8.19 (dd, *J* = 8.0 Hz, 1.5 Hz, 1H); 7.68 (ddd, *J* = 8.6 Hz, 7.1 Hz, 1.5 Hz, 1H); 7.54 (d, *J* = 16 Hz, 1H); 7.52 (dd, *J* = 8.6 Hz, 1.0 Hz, 1H); 7.39 (ddd, *J* = 8.0 Hz, 7.1 Hz, 1.0 Hz, 1H); 6.81 (s, 2H); 6.69 (d, *J* = 16 Hz, 1H); 6.36 (s, 1H); 3.94 (s, 6H); 3.90 (s, 3H). **¹³C NMR APT** (101 MHz, CDCl₃) δ 178.5; 161.9; 156.0; 153.6; 139.9; 137.2; 133.9; 130.6; 125.8; 125.1; 124.1; 119.6; 117.9; 110.5; 104.9; 61.1; 56.3. **HRMS** (M⁺·) 338.1161 (C₂₀H₁₈O₅)

Cytotoxicity screening on HeLa cells

Screening the cytotoxicity of synthesized compounds against HeLa cancer cells was carried out by the MTT method. This screening test was carried out at a concentration of 30 μM. The results were obtained with a single assay and are shown in Table 2. In the cytotoxicity screening, percent inhibition below 50% is declared as an inactive compound. Based on the results, there are some active compounds. The highest percentage of inhibition is held by compound **4g**, which had three methoxy substituents, increasing its activity against cancer cells. Previous research has explained that 2-styrylchromone compounds that have methoxy groups tend to be more active (Uesawa *et al.*, 2019).

Docking studies on Eg5 human kinesin protein

Nowadays, many studies have stated that Eg5 is a potential drug target for the development of cancer chemotherapy. The human kinesin Eg5 is responsible for bipolar spindle formation during early mitosis. Inhibition of Eg5 triggers the formation of monoastral spindles, leading to mitotic arrest that eventually causes apoptosis. There is increasing evidence that Eg5 constitutes a potential drug target for the development of cancer chemotherapeutics. The most sophisticated Eg5 targeting agent is ispinesib, which exhibits strong anticancer activity (Talapatra *et al.*, 2012). The selection of Eg5 protein in this study was based on the structure of ispinesib (Fig. 3). The two rings in

Table 2. Percent inhibitions result of cytotoxicity screening on HeLa cells.

Compound	% Inhibition
4a	91.4
4b	47.1
4c	71.6
4d	35.5
4e	87.6
4f	3.6
4g	100.1
Doxorubicin	101.2
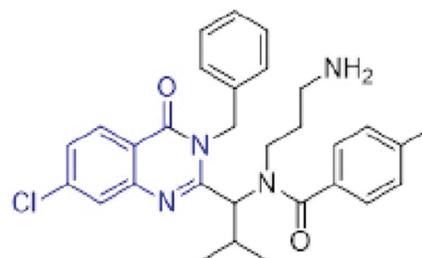
Figure 3. Structure of ispinesib.

the ispinesib structure are similar to the two rings A and C in the 2-styrylchromones structure.

In this study, molecular docking of synthesized compounds on the human kinesin Eg5 protein was carried out. The active side of the Eg5 protein is shown in Figure 4. Topological areas in red indicate hydrophobic regions, while topological areas in blue indicate hydrophilic regions.

Based on the figure, the binding cleft of the receptor tends to be hydrophobic residues. This can be seen from the amount of red around the ligand. Besides, it can be seen that ispinesib occupies the active side as a whole to carry out strong hydrophobic interactions with amino acid residues on the active site (Fig. 3b). This reasoning can also explain why the grid score (ΔG) of ispinesib is very low (−80.883560 kcal/mol). Meanwhile, the 2-styrylchromones showed the grid score values (ΔG) around −36 to −41 kcal/mol (Table 3). Table 3 presents the 2-styrylchromones-receptor interactions that occurred (3D visualization). Although the forming energy of 2-styrylchromones-receptor complexes is still higher than ispinesib receptor, negative and fairly low ΔG values indicate that complex formation can still occur spontaneously.

Table 2 and 3 show that compound **4g** was the most active among the synthesized compounds. However, it was less active when compared to the standard used (doxorubicin and ispinesib). Table 3 shows that compound **4g** does not fill the active side space of Eg5. This resulted in a weak interaction of the compound with the receptor. Figure 5 shows the 2D visualization of this interaction.

Momoi *et al.* (2005) established that compound **4g** showed higher cytotoxic activity against human tumor cell lines (squamous cell carcinoma HSC-2, HSC-3, submandibular gland carcinoma hysterosalpingogram, and promyelocytic leukemia HL-60) than against normal oral human cells (gingival fibroblast human gingival fibroblast, pulp cell human pulp cell, and periodontal ligament fibroblast human periodontal ligament fibroblasts). This compound induced internucleosomal DNA fragmentation in HL-60 cells which produced large DNA fragment in HSC-2 cells and enhanced the enzymatic activity to cleave the substrates for caspases 3, 8, and 9, suggesting the activation of both extrinsic and intrinsic apoptosis pathways.

The compound **4g** also exhibited significant potency against gastric carcinoma, HeLa, ovarian carcinoma (OVCA), hepatocellular carcinoma (SKHep), and H460 (large lung carcinoma) cell lines. The growth inhibition value shown by compound **4g** was always smaller than all synthesized compounds except for OVCA and SKHep cells, demonstrated by one substituted methoxy 2-styrylchromones. Compounds **4a**, **4b**, and **4c** were also synthesized in this study. According to the results in this study, the research conducted by Lin *et al.* (2013) also showed that compounds **4a**, **4b**, and **4c** exhibited lower activity than **4g**. However, compound **4g** was less active than doxorubicin, the same as shown in the results of this study.
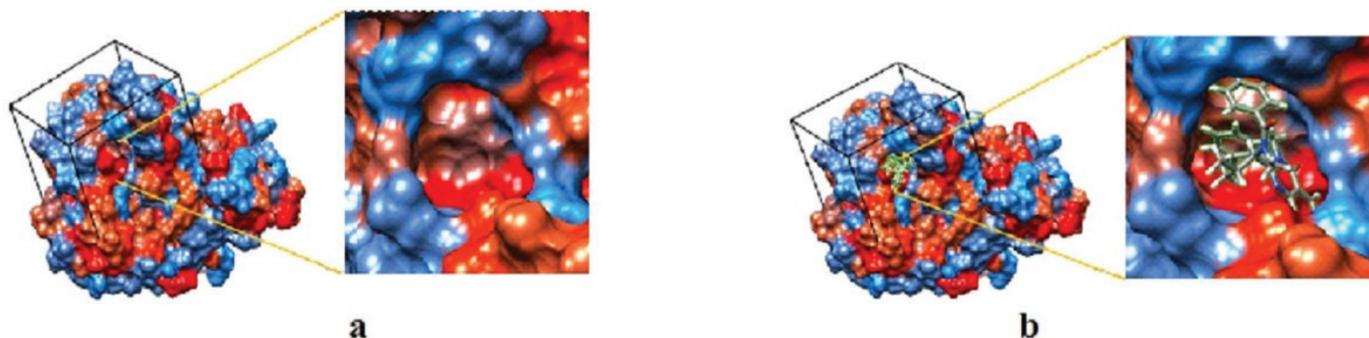
Figure 4. Binding cleft of Eg5 protein receptor (a) without ligand (b) with ispinesib ligand.

Table 3. The results of docking experiments of target molecules as ligands with Eg5 protein.

Ligan	*Gridscore* (kcal/mol)	Hydrogen bonding	Intermolecular interaction (Ligplot⁺)	Docking pose
Compound 4a	−38.701	Arg99 (2,81Å)	Arg99, Tyr191, Glu96, Ser212, Thr92, Arg201, Glu98, Gly97, Trp107	
Compound 4b	−36.802	–	Leu140, Glu96, Pro117, Arg99, Tyr191, Glu195, Leu194, Ala198, Arg201	
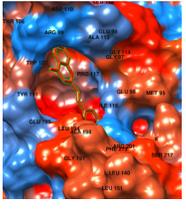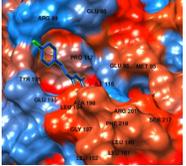
Continued

Ligan	*Gridscore* (kcal/mol)	Hydrogen bonding	Intermolecular interaction (Ligplot⁺)	Docking pose
Compound 4c	−37.805	–	Leu140, Glu96, Pro117, Ile116, Arg99, Leu194, Arg201	
Compound 4d	−37.406	–	Leu194, Pro117, Trp107, Tyr191, Gly97, Arg99, Glu98, Glu96	
Compound 4e	−37.635	Arg99 (2,89Å)	Leu194, Pro117, Tyr191, Trp107, Gly97	
Compound 4f	−38.676	–	Leu194, Pro117, Ala113, Arg99, Glu98, Gly97, Glu96, Arg201, Tyr191, Glu195	
Compound 4g	−41.029	–	Leu194, Pro117, Trp107, Tyr191, Gly97, Arg99, Glu98, Glu96	
Doxorubicin	−53.367	Tyr191 (3,11Å)	Leu194, Glu195, Ala198, Ala199, Thr202, Glu98, Gly97	
G7X (Ispinesib)	−80.883	-	Arg99, Tyr191, Gly197, Arg201, Leu151, Leu140, Leu194, Ile116, Glu96, Pro117, Trp107, Gly97, Val190, Glu98, Asp 110.	
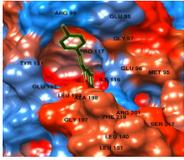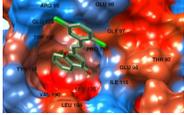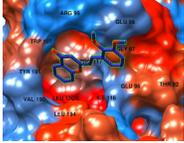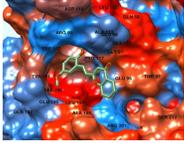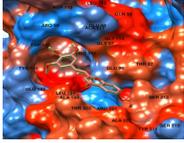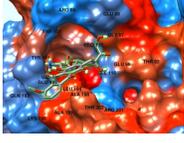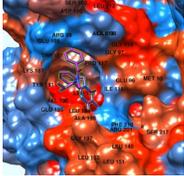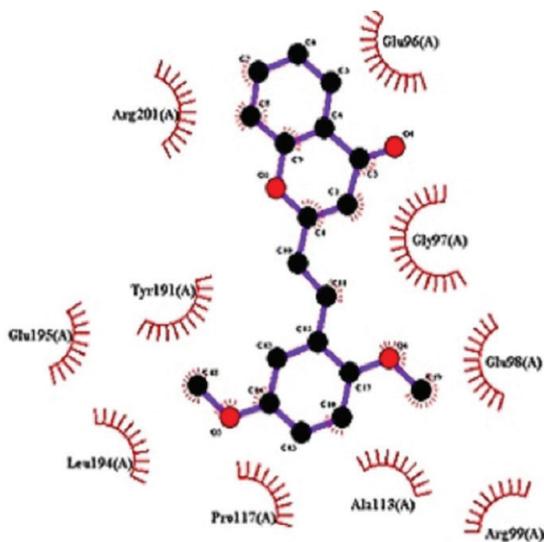
Figure 5. The 2D visualization of Eg5–compound **4g** interaction.

CONCLUSION

2-Styrylchromone derivatives can be synthesized using 2′-hydroxyacetophenone to produce 2-methylchromone, which formed 2-hydroxy-2-methylchromanone as an intermediate, followed by aldol condensation with benzaldehyde derivatives. The synthetic pathways obtained in this study were not the same as those previously reported. Between seven synthesized compounds, the most active compound was 2-stryrylchromone substituted by three methoxy groups, which was shown by both *in vitro* and *in silico* evaluations. 2-Styrylchromones substituted by more methoxy groups could be synthesized for further study to improve their anticancer activity.

ACKNOWLEDGMENTS

AUTHOR CONTRIBUTIONS

All authors made substantial contributions to conception and design, acquisition of data, or analysis and interpretation of data; took part in drafting the article or revising it critically for important intellectual content; agreed to submit to the current journal; gave final approval of the version to be published; and agree to be accountable for all aspects of the work.

CONFLICTS OF INTEREST

The authors report no conflicts of interest in this work.

FUNDING

ETHICAL APPROVAL

This study does not involve the use of animals or human subjects.

REFERENCES

Ali I, Lone MN, Aboul-Enein HY. Imidazoles as potential anticancer agents. Med Chem Commun, 2017; 8:1742–73.

Ali I, Lone MN, Al-Othman ZA, Al-WarthanA, Sanagi MM. Heterocyclic scaffolds: Centrality in anticancer drug development. Curr Drug Targets, 2015; 16(7):711–34.

Ali I, Saleem K, Wesselinova D, Haque A. Synthesis, DNA binding, hemolytic, and anti-cancer assays of curcumin I-based ligands and their ruthenium (III) complexes. Med Chem Res, 2013; 22:1386–98.

Bondge SP, Mahalle SR, Burungale AS, Patil LR, Mane RA. A facile synthesis of new 6-acetamido-3-aroyl-2-styryl chromones. Indian J Chem, 2009; 48B:1435–7.

Essien EE, Antia BS, Solomon AU, Choudhary MI. *In vitro* cytotoxic, antioxidant and antimicrobial activities of *Adoninia merrilli* and *Archontopheonix tukeri* fruit pericarps. Pharm Biosci J, 2016; 5(1):68–75.

Lin C, Lu P-J, Yang C-N, Hulme C, Shaw AY. Structure-activity relationship study of growth inhibitory 2-styrylchromones against carcinoma cells. Med Chem Res, 2013; 22:2385–94

Lu Z, Wu J, Liu W, Zhang G, Wang P. A ratiometric fluorescent probe for quantification of alkaline phosphatase in living cells. RSC Adv, 2016; 6:32046–51.

Momoi K, Sugita,Y, Ishihara M, Satoh K, Kikuchi H, Hashimoto K, Yokoe I, Nishikawa H, Fujisawa S, Sakagami H. Cytotoxic activity of styrylchromones against human tumor cell lines. In Vivo, 2005; 19:157–64.

Santos, CMM, Silva, AMS. An overview of 2-styrylchromones: natural occurrence, synthesis, reactivity and biological properties. Eur J Org Chem, 2017; 2017(22):3115–33.

Talapatra SK, Schüttelkopf AW, Kozielski F. The structure of the ternary Eg5–ADP–ispinesib complex. Acta Crystallogr D Biol Crystallogr, 2012; 68(10):1311–9.

Uesawa Y, Nagai J, Shi H, Sakagami H, Bandow K, Tomomura A, Sugita Y. Quantitative structure–cytotoxicity relationship of 2-styrylchromones. Anticancer Res, 2019; 39(12):6489–98.

Yadava U, Gupta H, Roychoudhury M. A comparison of crystallographic and DFT optimized geometries on two taxane diterpenoids and docking studies with phospholipase A2. Med Chem Res, 2011; 21(9):2162–8.

Zheng Y, Zhao M, Qinglong Q, Liu H, Lang H, Xu Z. A near-infrared fluorescent probe for hydrogen sulfide in living cells. Dyes Pigm, 2013; 98:367–71.